Journal of Power Sources 449 (2020) 227610

Contents lists available at ScienceDirect

Journal of Power Sources

journal homepage: www.elsevier.com/locate/jpowsour

Intragranular growth and evenly distribution mechanism of Li metal in $Li_7La_3Zr_2O_{12}$ electrolyte

L.C. Zhang [a], J.F. Yang [a,*], C.L. Li [a,b], Y.X. Gao [a], X.P. Wang [a], Q.F. Fang [a,b,**]

[a] Key Laboratory of Materials Physics, Institute of Solid State Physics, Chinese Academy of Sciences (CAS), Hefei, 230031, PR China
[b] University of Science and Technology of China (USTC), Hefei, 230026, PR China

HIGHLIGHTS

- Intragranular growth of lithium dendrite is firstly observed in garnet electrolyte.
- Lithium dendrite can be suppressed from electrolyte/Li interface with Au coating.
- A new lithium migration model is established.

ARTICLE INFO

Keywords:
Garnet
$Li_{6.55}La_{2.95}Ca_{0.05}Zr_{1.5}Ta_{0.5}O_{12}$
Solid electrolyte
Lithium dendrite
Short circuit

ABSTRACT

The application of garnet-type solid electrolytes in all-solid-state Li metal battery is seriously impeded by the lithium dendrite and resultant short-circuit. To explore its growth mechanism, in this work, a special asymmetric cell configuration is designed with a porous $Li_{6.55}La_{2.95}Ca_{0.05}Zr_{1.5}Ta_{0.5}O_{12}$ (LLCZTO) electrolyte between two mutually perpendicular Li metal strips. Besides the generally perceived lithium dendrite growth through grain boundaries, it is witnessed for the first time that lithium dendrite could also penetrate and break the LLCZTO grains, i.e., intragranular growth. Furthermore, uniform distributed lithium spherical particles, instead of lithium dendrite, are found on the surface of LLCZTO with Au-coating, demonstrating the beneficial effect of Au layer on restraining lithium dendrite growth. These findings shed new light on the growth mechanism and inhibition measures of lithium dendrite and would be helpful for the future research of all-solid-state Li metal battery with garnet-type solid electrolytes.

1. Introduction

$Li_7La_3Zr_2O_{12}$ (LLZO)-based garnet-type solid electrolytes have been considered as the potential candidate for all-solid-state Li metal battery, owing to the obvious advantages of high Li^+ conductivity of 10^{-3}–10^{-4} S cm^{-1} at room temperature, wide electrochemical potential window higher than 6 V, and relatively high stability against Li metal and ambient air [1–5]. However, the application has been significantly retarded by the lithium dendrite growth during lithium plating/stripping process as a result of the inhomogeneous and not-intimate contact in the Li/electrolyte interface with voids and asperities [6–8]. Although Li metal is soft and has a low melting temperature of 180 °C, it is still impossible to achieve the tight contact even under high pressure and/or at elevated temperature because of the poor wettability and non-negligible surface roughness [9].

Facing these challenges, several strategies have been adopted including surface coating on the electrolyte with Au [2,10,11], Al [12], C [13], Ge [14], Sn [15], Mg [16], Al_2O_3 [17] or ZnO [18], etc. The coating layers themselves or their reaction products with Li metal could work either as new electrode materials or buffer layer between the Li metal and electrolyte, which can enhance the lithium wettability, decrease the interfacial impedance and to a certain extent inhibit the lithium dendrite growth. Unfortunately, so far, the detailed Li^+ transport process as well as the growth mechanism of lithium dendrite are still mainly in the theoretical hypothesis stage. Although recent works have found that the lithium dendrite can be formed through either Li metal propagation along grain boundaries and interconnected pores or the reduction of Li^+ at the grain boundary inside electrolyte [2,7,8,19,20], however, the further understanding and more direct experimental evidences of continuous Li^+ migration path as well as the lithium

* Corresponding author. Key Laboratory of Materials Physics, Institute of Solid state Physics, Chinese Academy of Sciences, Hefei, 230031, China.
** Corresponding author. Key Laboratory of Materials Physics, Institute of Solid state Physics, Chinese Academy of Sciences, Hefei, 230031, China.
E-mail addresses: jfyang@issp.ac.cn (J.F. Yang), qffang@issp.ac.cn (Q.F. Fang).

https://doi.org/10.1016/j.jpowsour.2019.227610
Received 25 September 2019; Received in revised form 10 December 2019; Accepted 11 December 2019
Available online 13 December 2019
0378-7753/

dendrite growth are still urgently needed.

In this work, to elucidate the growth mechanism of lithium dendrite in garnet-type electrolyte $Li_{6.55}La_{2.95}Ca_{0.05}Zr_{1.5}Ta_{0.5}O_{12}$ (LLCZTO) and explore the possible measures to suppress them, the specially designed asymmetric cells with two mutually perpendicular Li metal strips as counter electrodes on both sides of the LLCZTO with or without Au-coating layer were employed and tested in combination with EIS, SEM and EDS techniques. We experimentally observed for the first time the intragranular growth of lithium dendrite inside LLCZTO electrolytes and the evenly distribution of Li metal on the Au-coating area. The Li^+ migration and distribution in the surface and interior of electrolytes were discussed.

2. Experimental

LLCZTO ceramic powder was synthesized as described in our previous work [21]. After ball-milling, the dried powder was firstly pressed into pellets and sintered at 700 °C for 20 h. Then the ball-milling and pressing processes were repeated. Finally, the pellets covered by the mother powder were sintered at 1100 °C for only 6 h to get a porous structure. The surface of the pellets was polished with 800, 1500 and 2000 grit SiC sandpapers, respectively. The final thickness of the pellets was about 1.40 mm to ensure mechanical strength, and the diameter was about 7.00 mm. Then, the Au layer with a diameter about 6.0 mm was formed on both sides of the pellets by using a sputter coater (K550X, Emitech) at the current of 20 mA for 60 s (Fig. S1).

All the cells were assembled in an Ar-filled glove box with the purity level of oxygen and moisture less than 0.1 ppm. The specially designed asymmetric Li–Au-LLCZTO-Au-Li cell was packed with an electrolyte pellet between two mutually perpendicular Li metal strips in the 2032-type coin cell. The Li metal strips with a width about 2.0 mm were cut down from the lithium foil, which had been scraped to remove the native oxide layer by blade and rolled by rolling mill in sequence. Two stainless steel (SS) plates with thickness about 0.3 mm were used in the cells on each side as spacer. For comparison, electrolytes without Au-coating were also used to assemble asymmetric cells noted as Li-LLCZTO-Li. All the cells were stored at 50 °C for at least 10H before testing.

The cells were cycled with a constant current of 0.022 mA and 1H plating/stripping time at 50 °C on a multi-channel battery test system (Neware, CT-4008). The electrochemical impedance spectroscopy (EIS) from 10 kHz to 1 Hz was measured on the electrochemical workstation (PARSTAT 4000, Princeton) at 50 °C. The conductivity of the LLCZTO pellet used in this work was measured at the temperature range from 30 to 110 °C with Au as blocking electrodes as shown in Fig. S2. The crystal structures of both sides of the polished electrolyte were characterized by X-ray diffraction (XRD, X'Pert, PANalytical) as shown in Fig. S3. After electrochemical test, the cells were disassembled inside glove box and then LLCZTO pellets were characterized by scanning electron microscopy (SEM) and energy dispersion spectrum (EDS) (SU8020, Hitachi).

3. Results and discussion

3.1. Intragranular growth of lithium dendrite in the short-circuited Li-LLCZTO-Li cell

Fig. 1a shows the EIS results of the Li-LLCZTO-Li and Li–Au-LLCZTO-Au-Li cells before cycling, both the two spectra present one incomplete semi-circle. The real axis values at the high frequency range corresponds to the total resistance of the LLCZTO electrolyte, the diameters of the semi-circle represent the interfacial resistance between the electrolyte and the Li metal [11]. According to the equivalent circuit shown in the inset of Fig. 1a and the fitting results of the Zview software (Table S1), the total resistance (R_0) values of the two cells were similar, and the constant phase element (CPE) values of the two cells were in the range of 10^{-7}–10^{-9} Fcm^{-2} which correspond to the reaction-diffusion process in the surface layer [22]. But the interfacial resistance (R_1) of the Li-LLCZTO-Li cell is about 45.7 KΩ, which dramatically drops to 6.6 KΩ in the cell with Au-coating. The decreased interfacial impedance should be attributed to the superior electrical conductivity of Au layer in the interface. During the lithium stripping/plating process of the Li-LLCZTO-Li cells without surface modification, short circuit easily happened, even at the first cycle as shown in Fig. 1b, while the Li–Au-LLCZTO-Au-Li cell went well at lower current densities (Fig. 1b and Fig. S4). The voltage of the Li–Au-LLCZTO-Au-Li cell kept stable at about 0.20 V during the constant dc measurement process, but the voltage of the Li-LLCZTO-Li cell increased rapidly to as high as 1.18 V at first, then reduced to 0.87 V gradually and finally dropped sharply to almost 0 V as the stripping/plating process went on (Fig. 1b). The initial high voltage implied a larger impedance, which are in good accordance with the EIS results (Fig. 1a). Then the dissolution and deposition of Li metal may further modify the interfacial contact to some extent and lead to the decrease of the impedance as well as the polarization voltage. But this process would not stop until the growth of lithium dendrite led to the short circuit.

To find out how this process was achieved, the failed Li-LLCZTO-Li cell was detached to get the electrolyte. Fig. 2a shows the cross-section SEM image and Fig. 2b is the enlarged map of the black frame, in which several irregular holes and a clear crack which started from the interior of the electrolyte and extended to the surface can be found. Both

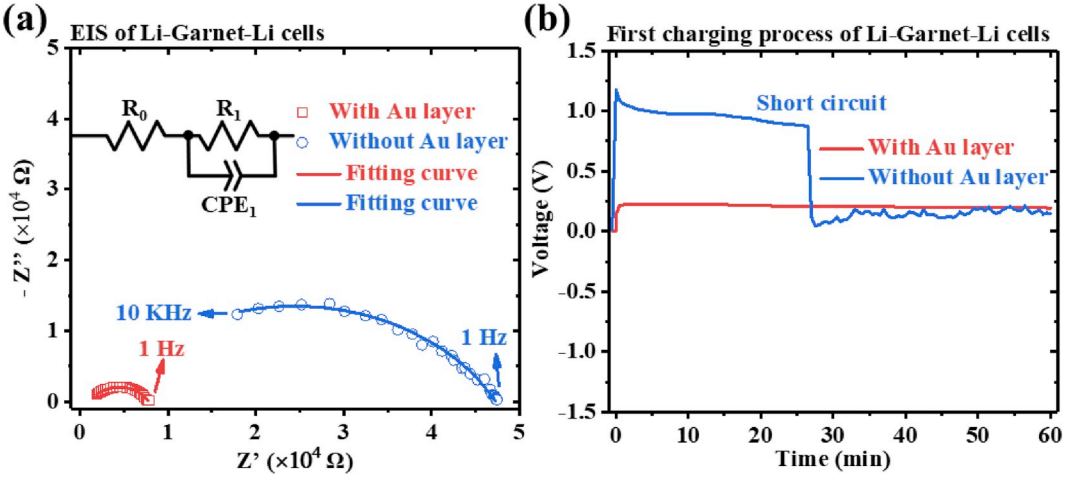

Fig. 1. (a) The EIS and the corresponding fitting curves of the Li–Au-LLCZTO-Au-Li and Li-LLCZTO-Li cells at 50 °C with the equivalent circuit shown in the inset. (b) The first charging process of the two cells with a constant dc of as high as 0.022 mA at 50 °C.

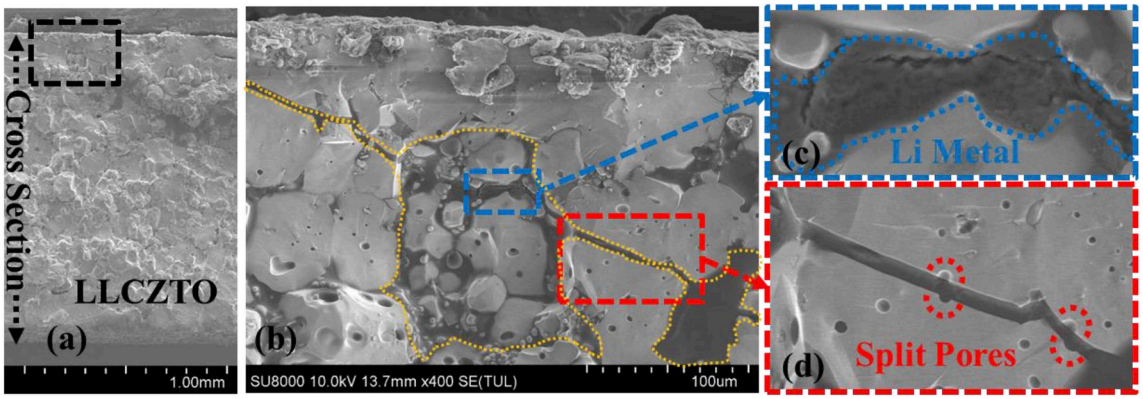

Fig. 2. (a) Cross-section SEM image of the Li-LLCZTO-Li cell after the short circuit happened, (b) The enlarged map of the black frame shown in (a), (c) and (d) are the detailed map of the blue and red frame shown in (b), respectively. (For interpretation of the references to colour in this figure legend, the reader is referred to the Web version of this article.)

the holes and crack are filled with Li metal, which is confirmed by the heat shrinkage phenomenon observed during the SEM test process as shown in Fig. 2c and Fig. S5. As marked in the yellow frame in Fig. 2b and the EDS results in Fig. S6, the crack was just like the "strait" between the "lithium oceans", and the continuous Li metal network with an irregular shape in the holes and crack has crossed one third of the cross-section of the electrolyte. It may be the very trigger and the direct evidence of the short circuit. Furthermore, it can be seen from Fig. 2d that two closed pores in the LLCZTO particle were split into two pairs of incomplete pores on both sides of the crack as indicated by two red dotted circles, which means that the separate two parts around the split pores used to be a whole. And the reason of the breaking could be the lithium dendrite, because the crack was filled with Li metal. A reasonable inference can be made that the deposited Li metal could induce the trans-crystalline fracture of the LLCZTO crystal particles. In this case, the prevention of Li metal local enrichment in the interface is particularly important. Once the lithium dendrite grew, it may pierce persistently into the electrolyte and finally lead to the short circuit as the mechanical strength of the electrolyte could not suppress it. In other words, facing the unmodified LLCZTO electrolyte, Li metal could always find a way.

Except for the Li metal observed in the interior of the electrolyte, it could also be found on the surface. Before the EDS test, the electrolyte was stored in dry air for a while for the Li metal to adequately react with CO_2. In this way, the in-situ formed carbonates may be used to indicate the distribution of Li metal. As shown in Fig. 3, Li metal may widespread on the surface in certain sites as point distribution (Fig. 3a) or some area as surface distribution (Fig. 3b) with SS as current collector. The detected Li metal should come from the deposition process rather than the external contamination because they were partly covered by several LLCZTO crystal particles as marked in the red frame in Fig. 3a, and the outline of the LLCZTO particles around by the Li metal is clear as shown in Fig. 3b. Remarkably, the Li metal could not distribute evenly on the surface, which should be the result of the incomplete contact between the electrolyte and the SS current collector. The decreased contact area would lead to an enhanced current density in the isolated sites, and to the locally concentrated Li metal distribution as well. Then the plated Li metal could work as a new current collector with low interfacial impedance and be apt to form the lithium dendrite growing into the electrolyte.

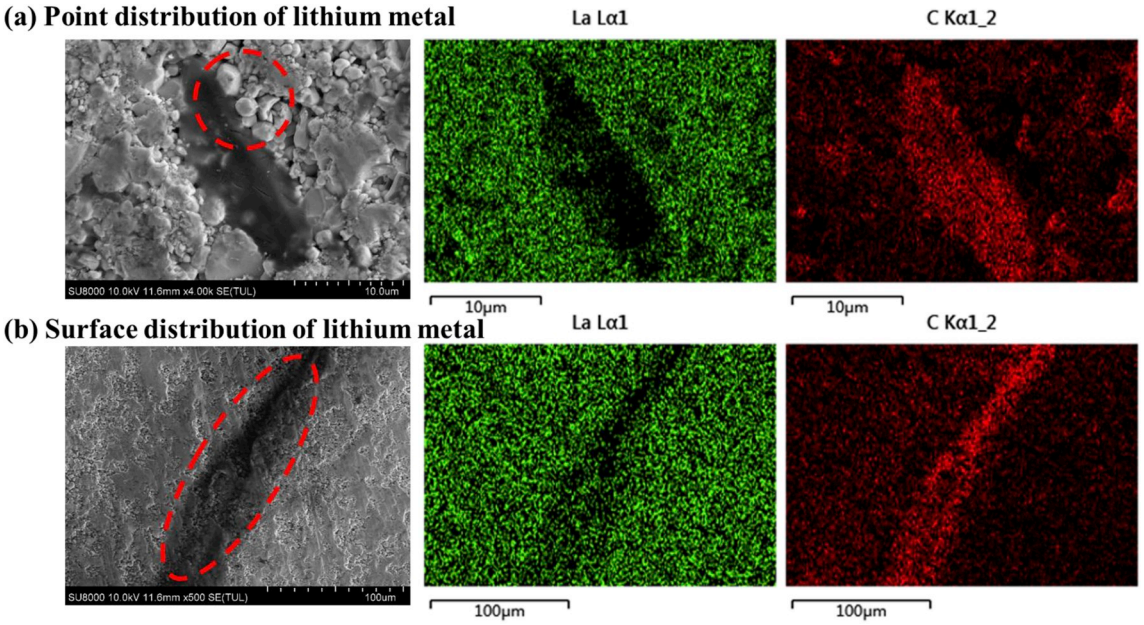

Fig. 3. SEM and EDS images of the surface of the electrolyte from failed Li-LLCZTO-Li cell with (a) a point distribution and (b) a surface distribution of Li metal.

3.2. Lithium dendrite prevention mechanism of Au-coating

Fig. 4a is the schematic illustration of the Li–Au-LLCZTO-Au-Li cell. The perpendicularly positioned Li strips were used for two reasons. Firstly, unlike the traditional cells with two face-to-face electrodes, the using of Li strips provide a chance to prove the possible lateral movement of the Li^+ by observing the blue frame area as shown in Fig. S7. Meanwhile, the deposition results in the opposite area of the Li metal electrode could also be observed (the red frame area in Fig. S7). Fig. 4b is the SEM image of the area around the Li metal strip as marked with red frame in Fig. 4a in which lots of spherical particles appeared on the surface of Au-coating area. By further observation, it can be seen that the spherical particles had smooth surfaces as shown in Fig. 4c and they had no direct relationship with the La, C or Au elements according to the EDS results. However, after being stored in dry air for several days, the surface changed to be rough as shown in Fig. 4d. And at this time, the particles had a strong relationship with the C element. Compared the two results shown in Fig. 4c and d, it can be concluded that the spherical particles should be the deposited Li metal. Due to the sample was tested immediately after being detached, so the spherical particles have a weak relationship with the C element in Fig. 4c. After reacting with CO_2 during storage in dry air, a strong relationship with C element could be shown in Fig. 4d.

Not only in the Au-coating area near the Li metal strips, but in the boundary region far away from the Li metal strips, lithium spherical particles also appeared in the Au-coating part, while the suspected Li metal aggregation appeared in the area without Au-coating layer as shown in Fig. 4e which is the enlarged map of the blue frame shown in Fig. 4a. Given the narrow Li metal strips electrodes and the asymmetric structure, it proved that the Li^+ could migrate along the vertical and transverse paths in the electrolyte and finally deposit uniformly on the whole Au-coating area no matter it is close to the lithium electrodes or not. In this case, no such lithium dendrite shown in Fig. 2 should grow in the Au-coating area. The well widespread lithium spherical particles could be used as the direct evidence of the homogenized distribution of electric field brought by the Au-coating layer and the lithium dendrite suppression mechanism of Au-coating layer.

3.3. Lithium migration mechanism in the internal and surface of LLCZTO electrolyte

According to the results above, the schematic diagrams of Li^+ migration and Li metal deposition were shown in Fig. 5. It is convinced that the Li^+ could transfer in the solid electrolyte along several vertical and transverse paths with similar impedance, just like a tree, as long as the counter side could provide electrons as described in Fig. 5a. The difference is that the Li metal particles tends to be evenly-distributed in the Au-coating area (Fig. 5b, Fig. 4b–e), while they were prone to be an aggregation in the area without Au-coating (Fig. 5b, Figs. 2, 3 and 4e). When the Li^+ was deposited on the surface, the whole Au-coating layer functions well as the electron conductor and the Li^+ could deposit anywhere in the Au-coating area. Therefore, the uniformly distributed

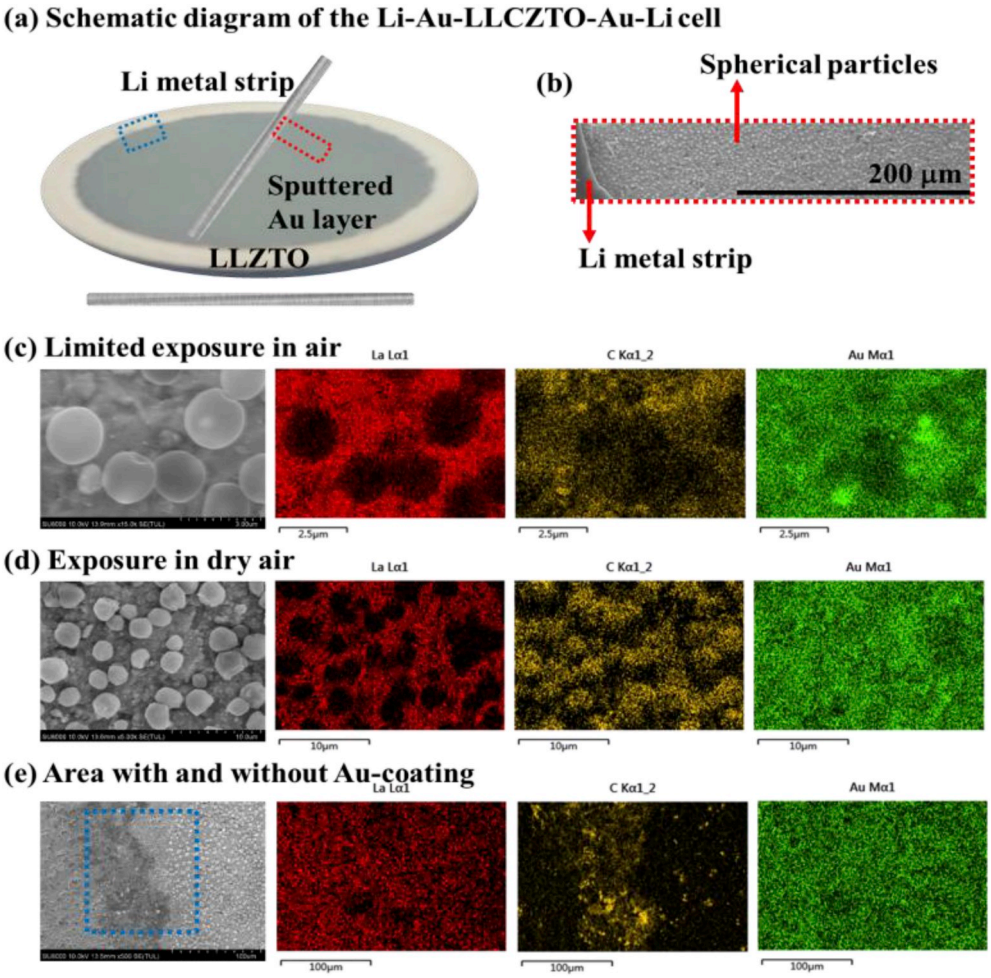

Fig. 4. (a) Schematic illustration of the Li–Au-LLCZTO-Au-Li cell. (b) The SEM image of the surface in the marked red frame region in (a). The SEM and EDS images of the spherical particles after just being detached (c) and stored in air for several days (d). (e) The SEM and EDS images of enlarged region shown as blue frame in (a). (For interpretation of the references to colour in this figure legend, the reader is referred to the Web version of this article.)

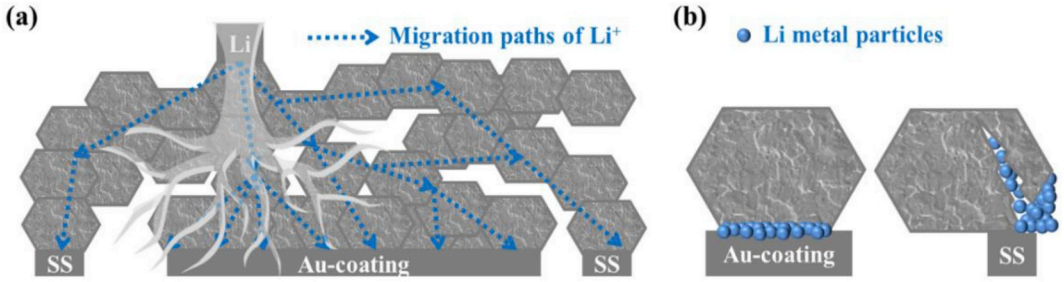

Fig. 5. (a) The schematic illustration of Li^+ migration in the solid electrolyte. (b) The schematic diagrams of the Li metal particles deposit in the surface of the electrolyte with and without Au-coating layer.

lithium spherical particles could be as the result of the homogenized distribution of electric field brought about by the Au-coating layer. In contrast, without Au-coating layer, the deposited Li metal could enrich in some places and have the possibility to grow along the boundaries as lithium dendrite. Moreover, another grim fact is that the lithium dendrite has the ability to create a way by breaking the LLCZTO particles as shown in Fig. 2. And the cracks could work as the new channels for lithium dendrite growth. It seems like that the lithium dendrite could always find a way in the solid electrolyte just like life. Therefore, it is extremely important to eliminate the lithium dendrite formation in the surface.

4. Conclusions

A long and continuous Li metal path was detected and used to analyze the growing process of lithium dendrite. The Li metal could not only deposit along the grain boundaries, but also break the LLCZTO particles. The result implies that once the lithium dendrite formed in the interface, it would not stop growing and piercing into the electrolyte till the short circuits happen. Although the result is unsatisfactory, the dendrite growth still could be suppressed by using surface Au-coating technique. The Au-coating layer could work as “a great wall” between the Li metal anode and the electrolyte, promote the uniform electric field distribution, and as a result, the evenly distribution of Li metal particles. In sum, the lithium dendrite could always find a way in the electrolyte and the only method to prevent it is to stop it in the surface. And fortunately, the proper Au-coating layer could achieve the goal to some extent and may be a promising method to deal with the interfacial issues of the future research of solid-state Li metal batteries with garnet solid electrolytes.

Declaration of competing interest

The authors declare that they have no known competing financial interests or personal relationships that could have appeared to influence the work reported in this paper.

Acknowledgements

This study was supported by National Key Research and Development Program of China (2017YFA0402800), China; National Natural Science Foundation of China (51502300, U1967211), China; Anhui Provincial Natural Science Foundation (Grant No.1608085QE88), China; and Hefei Center of Materials Science and Technology (2014FXZY006), China.

Appendix A. Supplementary data

Supplementary data to this article can be found online at https://doi.org/10.1016/j.jpowsour.2019.227610.

References

[1] A. Manthiram, X. Yu, S. Wang, Nat. Rev. Mater. 2 (2017), 16103.
[2] C.L. Tsai, V. Roddatis, C.V. Chandran, Q.L. Ma, S. Uhlenbruck, M. Bram, P. Heitjans, O. Guillon, ACS Appl. Mater. Interfaces 8 (2016) 10617–10626.
[3] Z.Z. Zhang, Y.J. Shao, B. Lotsch, Y.S. Hu, H. Li, J. Janek, L.F. Nazar, C.W. Nan, J. Maier, M. Armand, L.Q. Chen, Energy Environ. Sci. 11 (2018) 1945–1976.
[4] H.N. Duan, H.P. Zheng, Y. Zhou, B.Y. Xu, H.Z. Liu, Solid State Ion. 318 (2018) 45–53.
[5] K. Hofstetter, A.J. Samson, S. Narayanan, V. Thangadurai, J. Power Sources 390 (2018) 297–312.
[6] A. Jena, Y. Meesala, S.F. Hu, H. Chang, R.S. Liu, ACS Energy Lett. 3 (2018) 2775–2795.
[7] F. Aguesse, W. Manalastas, L. Buannic, J.M.L. del Amo, G. Singh, A. Llordes, J. Kilner, ACS Appl. Mater. Interfaces 9 (2017) 3808–3816.
[8] F. Han, A.S. Westover, J. Yue, X. Fan, F. Wang, M. Chi, D.N. Leonard, N.J. Dudney, H. Wang, C. Wang, Nat. Energy 4 (2019) 187–196.
[9] A.J. Louli, M. Genovese, R. Weber, S.G. Hames, E.R. Logan, J.R. Dahn, 166 (2019) A1291-A1299.
[10] G.V. Alexander, S. Patra, S. Valiyaveetil, S. Raj, M.K. Sugumar, M.M.U. Din, R. Murugan, J. Power Sources 396 (2018) 764–773.
[11] J. Wakasugi, H. Munakata, K. Kanamura, 164 (2017) A1022-A1025.
[12] Y. Lu, X. Huang, Y.D. Ruan, Q.S. Wang, R. Kun, J.H. Yang, Z.Y. Wen, J. Mater. Chem. 6 (2018) 18853–18858.
[13] Y.J. Shao, H.C. Wang, Z.L. Gong, D.W. Wang, B.Z. Zheng, J.P. Zhu, Y.X. Lu, Y. S. Hu, X.X. Guo, H. Li, X.J. Huang, Y. Yang, C.W. Nan, L.Q. Chen, ACS Energy Lett. 3 (2018) 1212–1218.
[14] W. Luo, Y.H. Gong, Y.Z. Zhu, Y.J. Li, Y.G. Yao, Y. Zhang, K. Fu, G. Pastel, C.F. Lin, Y.F. Mo, E.D. Wachsman, L.B. Hu, Adv. Mater. 29 (2017) 1606042–1606047.
[15] C.W. Wang, H. Xie, L. Zhang, Y.H. Gong, G. Pastel, J.Q. Dai, B.Y. Liu, E. D. Wachsman, L.B. Hu, Adv. Energy Mater. 8 (2018) 1701963–1701968.
[16] K. Fu, Y. Gong, Z. Fu, H. Xie, Y. Yao, B. Liu, M. Carter, E. Wachsman, L. Hu, 56 (2017) 14942-14947.
[17] X.G. Han, Y.H. Gong, K. Fu, X.F. He, G.T. Hitz, J.Q. Dai, A. Pearse, B.Y. Liu, H. Wang, G. Rublo, Y.F. Mo, V. Thangadurai, E.D. Wachsman, L.B. Hu, Nat. Mater. 16 (2017) 572.
[18] C.W. Wang, Y.H. Gong, B.Y. Liu, K. Fu, Y.G. Yao, E. Hitz, Y.J. Li, J.Q. Dai, S.M. Xu, W. Luo, E.D. Wachsman, L.B. Hu, Nano Lett. 17 (2017) 565–571.
[19] Y. Ren, Y. Shen, Y. Lin, C.-W. Nan, Electrochem. Commun. 57 (2015) 27–30.
[20] W. Manalastas, J. Rikarte, R.J. Chater, R. Brugge, A. Aguadero, L. Buannic, A. Llordés, F. Aguesse, J. Kilner, J. Power Sources 412 (2019) 287–293.
[21] L.C. Zhang, J.F. Yang, Y.X. Gao, X.P. Wang, Q.F. Fang, C.H. Chen, J. Power Sources 355 (2017) 69–73.
[22] J.T.S. Irvine, D.C. Sinclair, A.R. West, Adv. Mater. 2 (1990) 132–138.